RESEARCH ARTICLE

Ultrasound Breast Elastographic Evaluation of Mass-Forming Ductal Carcinoma-in-situ with Histological Correlation - New Findings for a Toothpaste Sign

Lester Chee Hao Leong[1]*, Llewellyn Shao-Jen Sim[1], Ana Richelia Jara-Lazaro[2], Puay Hoon Tan[3]

Abstract

 __Background:__ It is unclear as to whether the size ratio elastographic technique is useful for assessing ultrasound-detected ductal carcinoma-in-situ (DCIS) masses since they commonly lack a significant desmoplastic reaction. The objectives of this study were to determine the accuracy of this elastographic technique in DCIS and examine if there was any histopathological correlation with the grey-scale strain patterns. __Materials and Methods:__ Female patients referred to the radiology department for image-guided breast biopsy were prospectively evaluated by ultrasound elastography prior to biopsy. Histological diagnosis was the gold standard. An elastographic size ratio of more than 1.1 was considered malignant. Elastographic strain patterns were assessed for correlation with the DCIS histological architectural patterns and nuclear grade. __Results:__ There were 30 DCIS cases. Elastographic sensitivity for detection of malignancy was 86.7% (26/30). 10/30 (33.3%) DCIS masses demonstrated predominantly white elastographic strain patterns while 20/30 (66.7%) were predominantly black. There were 3 (10.0%) DCIS masses that showed had a co-existent bull's-eye sign and 7 (23.3%) other masses had a co-existent toothpaste sign, a strain pattern that has never been reported in the literature. Four out of 4/5 comedo DCIS showed a predominantly white strain pattern (p=0.031) while 6/7 cases with the toothpaste sign were papillary DCIS (p=0.031). There was no relationship between the strain pattern and the DCIS nuclear grade. __Conclusions:__ The size ratio elastographic technique was found to be very sensitive for ultrasound-detected DCIS masses. While the elastographic grey-scale strain pattern should not be used for diagnostic purposes, it correlated well with the DCIS architecture.

Keywords: Breast cancer - carcinoma-in-situ - elastographic evaluation - novel toothpaste sign

Introduction

The main principle behind the use of ultrasound strain elastography of the breast is that a malignant breast mass is generally harder than a benign one and shows less strain following compression. It has also been found that a malignant breast lesion appears larger on strain elastography than on conventional B-mode ultrasound imaging due to the presence of stiff tissue around the tumor. This is postulated to be related to the surrounding hard desmoplastic reaction (Leong et al., 2010; Garra et al., 1997; Hall et al., 2003) that is detected on elastography but not easily seen on B-mode imaging, therefore making the lesion appear bigger on elastography. A particular strain elastographic technique using size ratios uses this lesional size difference between elastography and B-mode imaging to help determine if a breast mass is malignant or benign.

In an earlier pilot study, we found that this size ratio elastographic technique was very sensitive for breast malignancy, even for the small number of ductal carcinoma-in-situ (DCIS) cases (Leong et al., 2010). However, it is well known that DCIS commonly lack significant desmoplastic reaction (Lester, 2010) and it is unclear if and why elastography will be useful in its diagnosis.

One of the objectives of this study was to expand from an earlier smaller study and specifically assess the sensitivity of detecting malignancy in DCIS masses using the size ratio ultrasound elastographic technique. The study also aimed to provide histological correlation for the elastographic grey-scale appearance of DCIS.

Materials and Methods

Patients

This study was approved by the hospital's Institutional

[1]*Diagnostic Radiology, Radiology,* [3]*Department of Pathology, Singapore General Hospital,* [2]*Quintiles East Asia Pte Ltd, Singapore*
For correspondence: lester.leong.c.h@sgh.com.sg

Review Board. Between September 2007 and February 2010, consecutive patients referred to the radiology department for image-guided core biopsies or hookwire localisations for surgical excisions that were not previously subjected to core biopsy were prospectively evaluated with elastography following informed consent. Only DCIS cases confirmed histologically after surgical excision were evaluated for this study. The study included the DCIS cases from the initial round of assessment conducted from September 2007 to March 2008 with the outcome published in 2010 (Leong et al., 2010) and additional cases evaluated from Apr 2008 to February 2010. Both rounds of assessment had a similar methodology.

Equipment

All studies were performed with a Siemens Antares ultrasound machine (Siemens Medical Solutions, Mountain View, CA, USA) which had both conventional B-mode ultrasound and elastography capabilities. The same 13MHz transducer probe was used for all the B-mode ultrasound and elastographic assessments.

Imaging Technique

Evaluation was carried out before the ultrasound-guided biopsies or hookwire localisation procedures were carried out. Each breast lesion was evaluated independently with conventional B-mode sonography and elastography by different radiologists who were blinded to each other's findings. Real-time elastographic assessment of the mass targeted for ultrasound-guided biopsy was performed by a radiologist before the biopsy procedure. The sonographers would obtain the B-mode images, which would be later retrieved from the picture archiving and communication system (PACS) and evaluated by another radiologist.

B-mode evaluation was assessed according to the Breast Imaging Recording and Data System (BIRADS). BIRADS scores of 2 and 3 were considered benign, whereas scores of 4 and 5 were considered malignant.

Elastography was performed by placing the ultrasound probe lightly on the breast surface, relying on gentle respiratory chest movements to provide mechanical compression on the breast lesion. There would be a dual live imaging screen on the ultrasound machine with the left-sided window showing the B-mode image and the right-sided window showing the elastographic image. Elastographic differentiation between a benign and a malignant breast mass was based on elastographic size ratio technique as evaluated by obtaining distance and area ratios. The distance ratio was defined as the maximum horizontal length of the lesion measured in the elastographic image divided by the corresponding length measured in the B-mode image. The area ratio was the area of the lesion measured in the elastographic image divided by the corresponding area measured in the B-mode image (Figure 1). The ratios were obtained in both the transverse and longitudinal planes and subsequently averaged to obtain the mean distance and mean area ratios. Mean distance and area ratios of less than or equal to 1.1 were predictive of benign pathology while mean ratios more than 1.1 were predictive of malignant

pathology. The cutoff ratio of 1.1 was chosen after it was found in our earlier study to be optimal for specificity while maintaining high sensitivity (Leong et al., 2010). In the event of discordance between the distance and area ratios, the most suspicious ratio would deem the lesion elastographically malignant.

Assessment of the elastographic grey-scale internal strain pattern was also performed and evaluated for histopathological correlation but was not used as a diagnostic criteria because it was previously shown to have a poor sensitivity (Leong et al., 2010). The grey scale refers to a range of grey shades between black and white generated by the elastogram software in the ultrasound machine that is mapped over the breast tissue. The scale represents the relative stiffness of tissues. The department's protocol assigned the range of darker shades to represent relative harder tissue and whiter shades to represent relatively softer issue. The main strain pattern categories were: homogeneous black (mass is almost completely black in colour), heterogeneous black with small white areas (more than 50% of the mass shows black colour), homogeneous white (mass is almost completely white) and heterogeneous white with small black areas (more than 50% of the mass is white). For the purpose of this study, homogeneous and heterogeneous black strain patterns were classified as predominantly black strain patterns which suggest most of the mass is hard. Similarly, homogeneous and heterogeneous white strain patterns were referred to as predominantly white strain patterns, which indicate that most of the mass is soft. In addition to the main strain patterns, the breast lesions were also assessed for the co-existence of two other special elastographic strain patterns, namely the bull's-eye sign and the toothpaste sign. The bull's-eye sign (Figure 2) is a well-documented, unique strain pattern which contains a white internal strain pattern accompanied by another white area located outside and posterior to the lesion. This white area seen posterior to the lesion is an elastographic artefact which is analogous to the posterior acoustic enhancement seen on ultrasound B-mode. This sign is useful in indicating a cyst or a cystic area (Barr RG et al., 2008). We also introduce a new strain pattern called the "toothpaste sign". This sign demonstrates a homogeneous, central, white tubular core with a black border which is similar to the appearance of toothpaste (Figure 3). It is possibly a variant of the bull's-eye sign but without the elastographic posterior enhancement. The toothpaste sign is classically tubular in appearance which is suggestive of a tubular duct involvement, hence it appears to be associated with ductal lesions.

There were 7 radiologists with 3 to 18 years of breast ultrasound imaging experience who provided conventional sonographic assessment. Three of them were dedicated breast radiologists who were involved the elastographic assessment arm of the study. The sonographers assisting in the study were dedicated breast sonographers with 5 to 15 years of breast ultrasound imaging experience.

Reference Standard

Histopathology was used as the reference standard and diagnosis of all DCIS cases based on standard criteria

US Breast Elastographic Evaluation of Mass-Forming Ductal Carcinoma-in-situ : Novel Toothpaste Sign

(Lakhani et al., 2012) were confirmed only from surgical specimens. Cases accompanied by established invasive carcinoma were excluded from the study. Surgical specimens and core biopsy samples, if available, were histologically evaluated for the presence of surrounding fibrosis or desmoplasia, DCIS architectural pattern and DCIS grade. The histological grade was based on nuclear features of lesional cells which were stratified into low, intermediate and high. Architectural patterns included cribriform, comedo, solid and papillary morphologies. Micropapillary type DCIS was grouped under papillary type DCIS in this study. In cases with two or more DCIS architectural patterns, the predominant architecture was selected for statistical analysis.

Statistical Analysis

Sensitivity for DCIS was assessed for B-mode and ultrasound elastographic imaging. The average elastographic distance and size ratios were calculated. The elastographic grey scale strain patterns were compared against the DCIS architecture and nuclear grade.

Continuous variables were compared using the Student's t-test. Comparisons of categorical variables were performed with the Fisher's exact test.

Statistical tests were performed with SPSS version 17 and Graphpad Quickcals.

Results

701 consecutive breast lesions from 586 women were evaluated with ultrasound elastography. Of these, there were 30 lesions of histologically proven DCIS without established invasive carcinoma from 28 women. 10 of the lesions were mammographically occult. Of the other 20 with abnormal mammogram findings, 4 lesions demonstrated abnormal microcalcifications, 13 presented as a mass or asymmetric density and 3 presented as mass with abnormal microcalcifications on mammography. The sensitivity for detection of malignancy in DCIS lesions was 80.0% (24/30) on ultrasound B-mode was and 86.7%

(26/30) on elastography (p=0.731). All 4 elastographic false negative cases were different cases from the false negative ones evaluated on B-mode imaging. Of these 4 false negative cases, 1 was of high nuclear grade while the other 3 were of intermediate nuclear grade. Average size of the DCIS masses was 13.7 ± 11.1 mm. The mean size of the true positive elastography cases was 14.6 ± 11.7mm while that of the false negative ones was 7.8 ± 2.2mm (p = 0.260).

Elastographic Size Ratio Assessment

The average elastographic distance ratio of DCIS was 1.35 ± 0.43 and the average size ratio was 1.56 ± 0.72. The mean distance and area ratios of the true positive cases are 1.41 ± 0.43 and 1.66 ± 0.73. All 4 false negative cases had size ratios of less than 1.1. The mean distance and area ratios of these false negative ones were 1.00 ± 0.11 (p = 0.072) and 0.93 ± 0.12 respectively (p = 0.061).
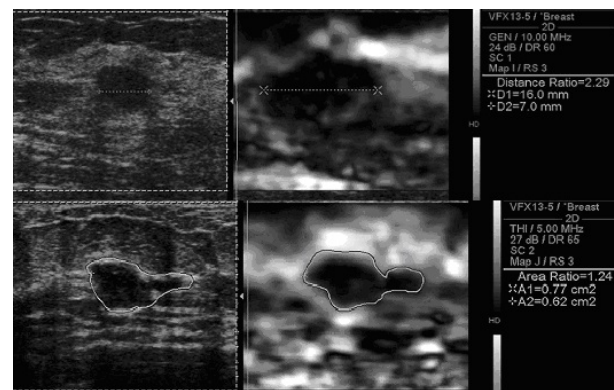
Figure 1. Illustration of the Size Ratio Elastographic Measurements in 2 Cases of Solid Type, Intermediate Grade DCIS. (Above) The distance ratio is the maximum horizontal distance of the lesion measured on elastography divided by the maximum horizontal distance measured in the B-mode image. (Below) For area ratio assessment, the outline of the lesion is manually traced on the elastogram image as well as on the B-mode image to obtain the areas. The elastogram area is then divided by the B-mode area to obtain the area ratio

Table 1. Relationship between Elastographic Strain Pattern and DCIS Architecture

		Predominant_architecture (%)			
		Papillary	cribriform	comedo	solid
Strain Pattern	Predominantly black	10 (66.7) *	3 (60.0)†	0 (0)	6 (100)
	Predominantly white	5 (33.3%)	2 (40.0)	4 (100.0)	0 (0)
	Total	15	5	4	6
	P-value	1	1	0.01	0.06

* Incidental tiny focus of papillary DCIS adjacent to a non-malignant intramammary lymph node, † One case of cribriform DCIS present in a non-malignant papilloma

Table 2. Correlation between the Presence of Bull's-eye and Toothpaste Signs with DCIS Architecture

		Predominant DCIS Architecture				Total	P-value
		Papillary	Cribriform	Comedo	Solid		
Bull's-eye	No	12 (44.4)	5 (21.7)	4 (17.4)	6 (26.1)	27	0.34
Sign (%)	Yes	3 (100)	0 (0)	0 (0)	0 (0)	3	
Toothpaste	No	8 (34.8)	5 (21.7)	4 (17.4)	6 (26.1)	23	0.03
Sign (%)	Yes	7 (100)	0 (0)	0 (0)	0 (0)	7	
Toothpaste and/or Bull's-eye	No	5 (21.7)	5 (21.7)	4 (17.4)	6 (26.1)	23	0.002
Sign (%)	Yes	10 (100)	0 (0)	0 (0)	0 (0)	10	

Table 3. Relationship between Elastographic Strain Pattern and DCIS Nuclear Grade

		DCIS Nuclear Grade (percentage %)			P value
		High	Intermediate	Low	
Strain Pattern	Predominantly Black	2 (28.6)	12 (70.6)	5 (83.3)	
	Predominantly White	5 (71.4)	5 (29.4)	1 (16.7)	0.08
	Total	7	17	6	

Table 4. Correlation between the Presence of the Bull's-eye and Toothpaste Signs with DCIS Nuclear Grade

		DCIS Nuclear Grade			Total	P-value
		High	Intermediate	Low		
Bull's-eye Sign (%)	No	7 (25.9)	14 (51.9)	6 (22.2)	27	0.28
	Yes	0 (0)	3 (100)	0 (0)	3	
Toothpaste Sign (%)	No	6 (26.1)	14 (60.9)	3 (13.0)	23	0.22
	Yes	1 (14.3)	3 (42.9)	3 (42.9)	7	
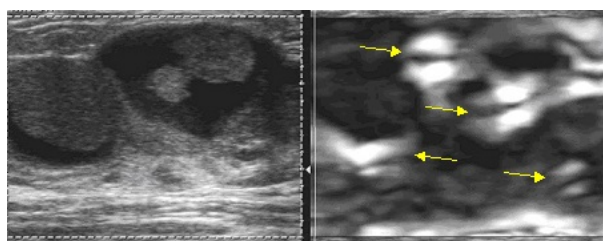
Figure 2. Intracystic Papillary Carcinoma Displaying Multiple Bull's-Eye Signs (Yellow Arrows). The cystic areas show multiple white areas with artefactual "posterior elastographic enhancement" on elastography (right) while the solid parts of the lesion show a predominantly black strain pattern. This shows that the presence of the bull's-eye sign may not necessarily indicate a benign lesion
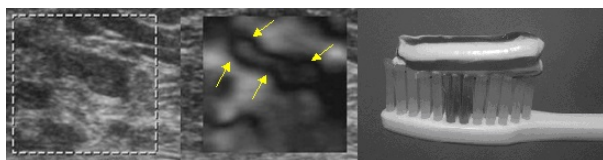
Figure 3. Low grade, papillary DCIS Showing the Toothpaste Sign. Elastography shows a soft, white, tubular core with a black margin

*Elastographic Grey Scale Strain Pattern Assessment*

Eleven (36.7%) DCIS lesions demonstrated a predominantly white strain pattern while

19 (63.3%) had a predominantly black strain pattern. (Table 1) There were 3 (10.0%) DCIS masses that showed the bull's-eye sign and another 7 (23.3%) that displayed the toothpaste sign.

All 4 comedo DCIS showed a predominantly white strain pattern (p = 0.012). Majority of the papillary (10/15, p = 1.000), cribriform (3/5, p = 1.000) and solid (6/6, p = 0.061) DCIS showed predominantly black strain patterns (Table 1). All the cases demonstrating the bull's-eye and toothpaste signs were related to papillary DCIS (p = 0.002) (Table 2).

Histological Assessment

All 26 cases that were positive on elastography showed moderate to marked degree of fibrosis, stromal alteration and distortion around the DCIS cells and affected ducts
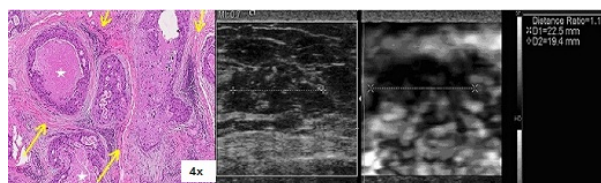
Figure 4. (Histology and Elastography of Comedo DCIS. (Left) Histology of high grade, comedo DCIS shows significant stromal reaction and distortion (yellow arrows) surrounding the DCIS cells (H&E stain, x4). White star areas indicate pools of comedo necrosis within the ducts. (Right) The elastographic size ratio for this DCIS mass was found to be greater than 1.1 and there was a heterogeneous white strain pattern. The white areas could be
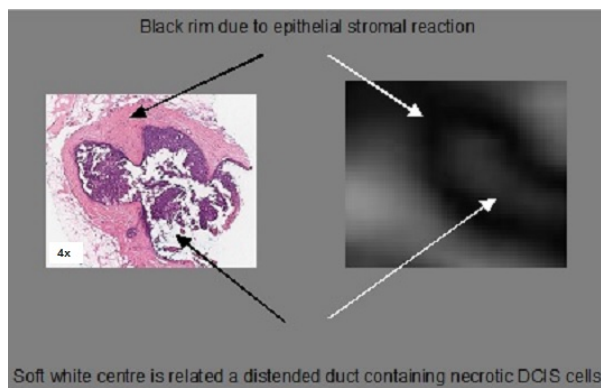
Figure 5. Histological Correlation for the Toothpaste Sign in a Case of Papillary DCIS (H&E stain, x4). In this example, the soft white center seen on elastography (right) correlated with a centrally distended duct that contained necrotic cells (left). The black rim enveloping the central white area may be explained by the stromal reaction surrounding the DCIS cells

on histology (Figure 4). The 4 false negative DCIS cases either did not show any significant stromal changes or demonstrated only minimal peripheral fibrosis on histological review. One of the false negative cases was actually a small intramammary lymph node with an incidental adjacent finding of a tiny focus of papillary DCIS (predominantly black strain pattern). The other 3 false negative cases were related to a comedo (white strain pattern), a cribriform (white strain pattern) and a solid (black strain pattern) type DCIS architecture.

The necrosis in the comedo DCIS cases were found in several prominent ducts. For the solid DCIS cases, 1 of the cases had co-existent, small areas of comedo necrosis while the other 5 had small, co-existent cribriform DCIS. However, the dominating histological picture was that of cells filling several ducts in keeping with a predominantly solid type DCIS. Ducts associated with papillary and cribriform DCIS had variable luminal duct spaces. Of the 3 cases demonstrating the bull's-eye sign, 1 was found in an intracystic papillary DCIS which contained cystically dilated ducts while the other 2 had prominent cystic spaces within the papillary DCIS masses. All 7 cases with the toothpaste sign had distended ducts with possible ductal debris or haemorrhage. Prominent stromal fibrosis was also seen around the affected distended ducts in the cases exhibiting the bull's-eye and toothpaste signs (Figure 5). There was no relationship between the strain patterns and the DCIS nuclear grade (p = 0.080) (Table 3).

Discussion

DCIS is pre-invasive cancer, composed of malignant epithelial cells derived from the terminal duct-lobular unit of the breast with no demonstrable invasion through the basement membrane. It is mostly detected as a result of abnormal mammographic microcalcifications. However, up to 22% of DCIS can present without microcalcifications and as many as 44% of DCIS cases are mammographically occult (Dershaw et al., 1989; Stomper et al., 1989; Ikeda and Andersson, 1989; Kuhl et al., 2007), detected only on ultrasound examination or MRI. There are a few explanations for DCIS appearing as masses. DCIS can elicit a sclerosing and fibrotic stromal response with an inflammatory lymphocytic infiltrate, encapsulating the DCIS and forming a mass. Formation of an encapsulated papillary carcinoma with a cystically dilated duct is also another cause of a mass-forming DCIS. Lastly, if the DCIS involves a pre-existing mass like a fibroadenoma or a papilloma, it can appear as a mass, although in itself, the DCIS is not mass-forming. While the sonographic appearances of DCIS have been well documented (Moon et al., 2002; Gwak et al., 2011, Uematsu, 2012), a detailed analysis of the ultrasound elastographic appearance is lacking. To our knowledge, no article has evaluated the elastographic appearance of DCIS with direct histological correlation which this article hopes to demonstrate.

As DCIS does not have an invasive component, it rarely elicits significant surrounding desmoplastic reaction except in comedo DCIS (Lester, 2010). This makes it doubtful if the elastographic size ratio technique would be useful in the sonographic diagnosis of DCIS if there is a lack of surrounding desmoplasia for elastographic images to appear larger than B-mode images. However, most of these ultrasound-detected DCIS masses are by default, forming a mass as a result of stromal fibrosis or desmoplasia enveloping the DCIS. Our study found this to be mostly true. In all 26 DCIS masses that were positive on elastography, there were significant fibrosis and stromal disturbance around the DCIS cells. The converse was also true. The 4 DCIS cases that were negative on elastography did not show any significant stromal changes. One of these false negative cases was actually a tiny incidental nest of DCIS found next to a non-malignant lymph node and the mass visualised on B-mode and elastography was probably related to the lymph node rather than the DCIS focus. However, it is unclear for now, as to why the other 3 cases did not show significant stromal changes. Nevertheless, the histological findings do strongly indicate that mass-forming DCIS mostly show surrounding stromal changes which are helpful for the size ratio elastographic technique.

The results showed that the size ratio elastographic criterion is reasonably sensitive for DCIS. There were 3 false negative cases were actually found to be suspicious and categorized as BIRADS 4 on B-mode imaging assessment. In clinical practice, these lesions would undergo combined B-mode and elastographic assessment and would potentially be identified for further histological evaluation due to its suspicious appearance on B-mode imaging despite being negative on elastography. On the other hand, elastography was positive for the other 6 cases that were thought to be negative on B-mode imaging. Hence, in the combined sonographic assessment of breast masses, elastography can help increased the sensitivity, especially for those borderline BIRADS 3/4A lesions. In addition, one of the false negative cases was actually a small intramammary lymph node with an incidental adjacent focus of DCIS as explained above. As such, the actual sensitivity should be 89.7% (26/29) due to one less false negative case.

The use of the size ratio cutoff of 1.1 instead of 1.0 did not result in several false negatives. An analysis of the false negative cases showed that using a cutoff ratio of 1.1 would probably not make much of a difference to overall sensitivity as only 1 out of the 4 false negative cases had size ratios that were marginally higher than 1.0. The majority of the DCIS masses on the other hand, had size ratios that were significantly greater than 1.1. As also shown in our earlier work, this higher cutoff value would not result in the significant compromise of malignancy detection, and it would also afford the advantage of having a better specificity of approximately 70% (Leong et al., 2010).

Histological evaluation was able to show correlation between the grey scale strain patterns and the DCIS architecture. Significant areas of necrosis could account for the predominantly white and soft strain pattern found in all the comedo DCIS cases. All the solid type DCIS had other types of DCIS present but the predominant finding of solid DCIS cells filling the duct spaces probably explained the black strain patterns. In most of the papillary and cribriform DCIS, the cystic and luminal duct spaces appear generally small, which may explain why they were generally black and hard on strain imaging. However, the size of the luminal and glandular spaces were quite variable but it was possible that those with bigger spaces might have given rise to white areas on strain imaging. In the cases demonstrating the bull's-eye or the toothpaste sign, histology was able to demonstrate moderately distended or dilated ducts surrounded by papillary DCIS cells in all of these cases. The dilated ducts and their predominantly cystic contents would explain the white,

Lester Leong et al

soft internal areas seen in the bull's-eye sign. This also shows that the presence of the bull's-eye sign is not necessarily indicative of benignity. For the toothpaste sign, the prominent ducts did not seem to cause any artefactual posterior elastographic enhancement as seen in the bull's-eye sign. We observed that these distended ducts appeared to contain some residual cells and debris on histological review. It is possible that the ducts were filled with material denser than fluid such as blood products, necrotic material and cellular debris. The mixed solid-cystic ductal contents remained relatively soft but would still be dense enough to limit the acoustic transmission of ultrasound and any posterior elastographic enhancement. Another component of the toothpaste sign consists of the black rim that encircles the lesion on elastography. The hard stromal reactive tissue around the DCIS mass would probably account for this elastographic appearance at the periphery of the lesion (Figure 5).

The strain pattern findings also showed that a fairly significant number of slightly more than a third of the DCIS masses displayed predominantly white and soft internal strain patterns. The presence of the white internal strain pattern, therefore, cannot exclude malignancy and this reinforces the earlier evidence that strain pattern evaluation is unreliable and should not be used for diagnostic assessment. This may also explain why the other elastographic techniques such as the colour scoring method and shearwave elastography are not as useful for DCIS if they only assess for internal tissue stiffness, which this study has shown, can be soft in some of the DCIS masses. The well-documented colour scoring method (Matsumura et al., 2004; Itoh et al., 2006) is a qualitative type, pattern-based, strain elastography scoring assessment which has a reported sensitivity of 50-71% for DCIS (Itoh et al., 2006; Tan et al., 2008; Sohn et al., 2009). Shearwave elastography, which measures the speed of shearwaves within the tissue to quantify its stiffness, has a reported sensitivity of 56-60% (Chang et al., 2013; Vinnicombe et al., 2014). These papers had small sample sizes of less than 10 cases of DCIS each but the results seem to suggest that the size ratio technique may be more accurate than the other elastographic techniques.

The study has a small sample size. This is mainly because mass-forming DCIS detected on sonography is not a common finding. Nevertheless, the 30 cases in this study provide one of the largest series on ultrasound elastographic assessment of DCIS masses. The prevalence of the toothpaste sign in other types of breast lesions is also uncertain and this sign may not be specific for DCIS. However, from our observation, the toothpaste sign appears to be related to intraductal breast lesions. That may explain why it appears in DCIS. It is possible that it may be seen in other intraductal lesions such as papillomas. A larger study involving elastographic evaluation of all other types of breast lesions is being carried out to determine its prevalence and relevance.

In conclusion, the size ratio elastographic technique was found to be sensitive for ultrasound-detected DCIS masses. The elastographic grey-scale strain pattern, however, was not accurate for evaluation of breast malignancy, but could correlate with the DCIS architecture. The bull's-eye and toothpaste strain pattern signs also correlated with papillary DCIS. Larger scientific studies are needed to further validate these findings.

References

Barr RG, Campbell, Grajo JR (2008). Sensitivity and specificity of the bull's-eye artifact on breast elastography imaging to characterize cysts. 2008 RSNA Scientific Assembly.

Chang JM, Won JK, Lee KB, et al (2013). Comparison of shear-wave and strain ultrasound elastography in the differentiation of benign and malignant breast lesions. *AJR Am J Roentgenol*, **201**, 347-6.

Dershaw DD, Abramson A, Kinne DW (1989). Ductal carcinoma in situ: Mammographic findings and clinical implications. *Radiology*, **170**, 411–5.

Garra BS, Cespedes EI, Ophir J, et al (1997). Elastography of breast lesions: initial clinical results. *Radiol*, **202**, 79-6.

Gwak YJ, Kim HJ, Kwak JY, et al (2011). Ultrasonographic detection and characterization of asymptomatic ductal carcinoma in situ with histopathologic correlation. *Acta Radiol*, **52**, 364–1.

Hall T, Svensson W, Von Behren P, et al (2003). Lesion Size Ratio for Differentiating Breast Masses. *IEEE Ultrasonics Symposium*, **2**, 1247-0.

Ikeda DM, Andersson I (1989). Ductal carcinoma in situ: Atypical mammographic appearances. *Radiol*, **172**, 661–6.

Itoh A, Ueno E, Tohno E, et al (2006). Breast disease: clinical application of US elastography for diagnosis. *Radiol*, **239**, 341–0.

Kuhl CK, Schrading S, Bieling HB, et al (2007). MRI for diagnosis of pure ductal carcinoma in situ: a prospective observational study. *Lancet*, **370**, 485-2.

Lakhani, SR, Ellis, IO, Schnitt SJ, Tan PH, van de Vijver M (2012). World Health Organisation Classification of Tumours of the Breast, IARC, Lyon.

Leong LC, Sim LS, Lee YS et al (2010). A prospective study to compare the diagnostic performance of breast elastography versus conventional breast ultrasound. *Clin Radiol*, **65**, 887-4.

Lester S (2010). Manual of surgical pathology. 3rd edition. in: breast. philadelphia: saunders. 262-8.

Matsumura T, Tamano S, Shinomura R, et al (2004). Preliminary evaluation of breast disease diagnosis based on real-time elasticity imaging. In proceedings of the third international conference on the ultrasonic measurement and imaging of tissue elasticity. Lake Windermere: Cumbria, United Kingdom, 17e20, 023.

Moon WK, Myung JS, Lee YJ, et al (2002). US of ductal carcinoma in situ. *Radiographics*, **22**, 269-0.

Stomper PC, Connolly JL, Meyer JE, et al (1989). Clinically occult ductal carcinoma in situ detected with mammography: Analysis of 100 cases with radiologic-pathologic correlation. *Radiol*, **172**, 235-1.

Sohn YM, Kim MJ, Kim EK, et al (2009). Sonographic elastography combined with conventional sonography: how much is it helpful for diagnostic performance? *J Ultrasound Med*, **28**, 413-0.

Tan SM, Teh HS, Mancer JF, Poh WT (2008). Improving B mode ultrasound of breast lesions with real-time ultrasound elastography: a clinical approach. *Breast*, **17**, 252–7.

Uematsu T (2012). Non-mass-like lesions on breast ultrasonography: a systematic review. *Breast Cancer*, **19**, 295-1.

Vinnicombe SJ, Whelehan P, Thomson K, et al (2014). What are the characteristics of breast cancers misclassified as benign by quantitative ultrasound shear wave elastography? *Eur Radiol*, **24**, 921-6.